ANTICANCER RESEARCH *40*: 4885-4894 (2020)
doi:10.21873/anticanres.14491

Antitumor Effects and Tumor-specificity of Guaiazulene-3-Carboxylate Derivatives Against Oral Squamous Cell Carcinoma *In Vitro*

MICHITO TERATANI[1], SHOUTA NAKAMURA[1], HIROSHI SAKAGAMI[2], MASAKAZU FUJISE[1], MASASHI HASHIMOTO[1], NORIYUKI OKUDAIRA[3], KENJIRO BANDOW[4], YOSUKE IIJIMA[5], JUNKO NAGAI[6], YOSHIHIRO UESAWA[6] and HIDETSUGU WAKABAYASHI[1]

[1]*Faculty of Science, Josai University, Saitama, Japan;*
[2]*Meikai University Research Institute of Odontology (M-RIO), Saitama, Japan;*
[3]*Department of Biochemistry, Teikyo University School of Medicine, Tokyo, Japan;*
[4]*Division of Biochemistry, Meikai University School of Dentistry, Saitama, Japan;*
[5]*Department of Oral and Maxillofacial Surgery, Saitama Medical Center, Saitama Medical University, Kawagoe, Japan;*
[6]*Department of Medical Molecular Informatics, Meiji Pharmaceutical University, Tokyo, Japan*

Abstract. *Aim: The aim of this study was to investigate the antitumor potential of guaiazulene-3-carboxylate derivatives against oral malignant cells. Materials and Methods: Twelve guaiazulene-3-carboxylate derivatives were synthesized by introduction of either with alkyl group [**1-5**], alkoxy group [**6, 7**], hydroxyl group [**8, 9**] or primary amine [**10-12**] at the end of sidechains. Tumor-specificity (TS) was calculated by the ratio of mean 50% cytotoxic concentration (CC_{50}) against 3 human oral mesenchymal cell lines to that against 4 human oral squamous cell carcinoma (OSCC) cell lines. Potency-selectivity expression (PSE) was calculated by dividing TS value by CC_{50}value against OSCC cell lines. Cell cycle analysis was performed by cell sorter. Results: [**6, 7**] showed the highest TS and PSE values, and induced the accumulation of both subG_1 and G_2/M cell populations in HSC-2 OSCC cells. Quantitative structure-activity relationship analysis demonstrated that their tumor-specificity was correlated with chemical descriptors that explain the 3D shape, electric state and ionization potential. Conclusion: Alkoxyl guaiazulene-3-carboxylates [**6, 7**] can be potential candidates of lead compound for developing novel anticancer drugs.*

This article is freely accessible online.

Correspondence to: Hidetsugu Wakabayashi, Faculty of Science, Josai University, 1-1 Keyakidai, Sakado, Saitama 350-0295, Japan. Tel: +81 492717963, Fax: +81 492717985, e-mail: hwaka@josai.ac.jp, sakagami@dent.meikai.ac.jp

Key Words: QSAR, guaiazulene-3-carboxylate, OSCC, tumor-specificity, molecular shape, ionization potential.

Azulene (Figure 1A) is an isomer of naphthalene having a dipole moment and a resonance energy with intermediate values between that of benzene and naphthalene; it is considerably more reactive, when compared with these two arenes (1-4). Among the 962 papers cited in PubMed regarding azulenes, most of them have focused on its chemistry, followed by biological activity, while few papers have focused on dentistry and oral application. Sodium azulene sulfonates have been reported to be effective for the treatment of oral mucositis (5) and oral lichen planus (6), possibly due to their antioxidant and anti-inflammatory activities (7, 8). In contrast, much reduced numbers of papers of guaiazulene (Figure 1B), a lipophilic azulene derivative, have been published, approximately half of which have dealt with its chemistry. Guaiazulenes also have antioxidant and anti-inflammatory activities (9-11) and a few papers have dealt with the treatment of oral diseases (12, 13).

As far as we know, anticancer potential of guaiazulene derivatives against human oral malignant cells has not yet been reported. This urged us to initiate the investigation of 10 alkylaminoguaiazulenes (Figure 1C) (14), 10 guaiazulene amides (Figure 1D) (15) and 14 azulene amide derivatives without or with 7-isopropylgroup (Figure 1E, F) (16). We have reported that the introduction of an isopropyl group in the seven-member ring and an amide group rather than alkylamino group in the five-member ring of guaiazulene increased the specific cytotoxicity against malignant cells over non-malignant cells (14-16) (Figure 1). Furthermore, quantitative structure-activity relationship (QSAR) analyses demonstrated the tight correlation of their tumor-specificity with hydrophobicity and molecular shape (15, 16).

The aim of the present study was to search for more tumor-selective guaiazulene derivatives. For this purpose, we

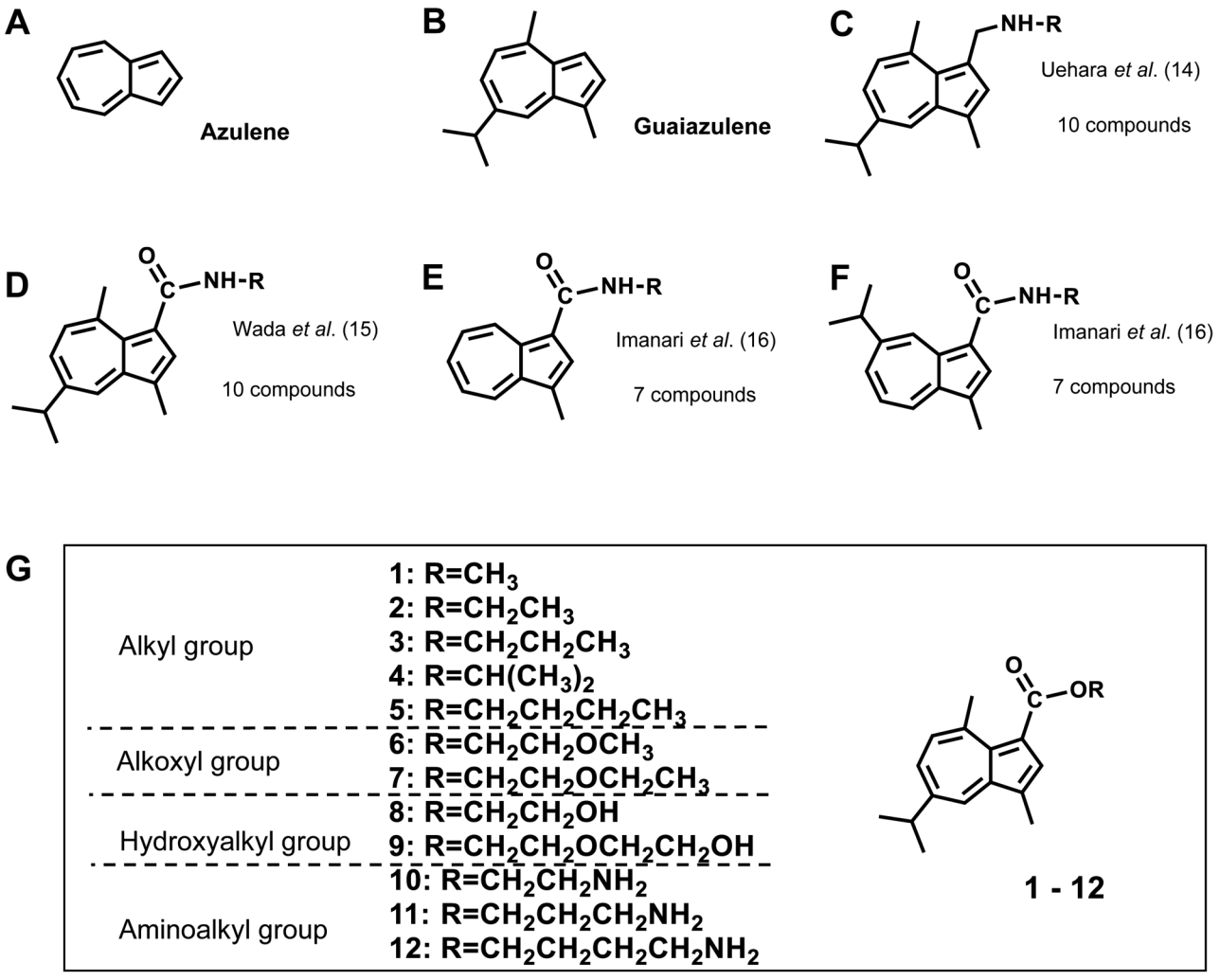

Figure 1. *Structure of azulene (A), guaiazulene (B), alkylaminoguaiazulenes (C), guaiazulene amides (D), azulene amide derivatives without (E) or with 7-isopropylamino group (F), and 12 guaiazulene-3-carboxylate derivatives used in this study (G).*

synthesized a total of 12 guaiazulene-3-carboxylate derivatives [**1-12**] (Figure 1), in which alkyl group [**1-5**], alkoxy group [**6, 7**], hydroxyl group [**8, 9**] and primary amine [**10-12**] were introduced at the end of sidechain (Figure 1G), and investigated their tumor-specificity using four human oral squamous cell carcinoma (OSCC) cell lines and three human normal oral cells. We also investigated the effects of these compounds on cell cycle phase distribution, in OSCC cells.

Materials and Methods

Materials. The following chemicals were obtained from the indicated companies: Dulbecco's modified Eagle's medium (DMEM) from Gibco BRL, Grand Island, NY, USA); fetal bovine serum (FBS), 3-(4,5-dimethylthiazol-2-yl)-2,5-diphenyltetrazolium bromide (MTT) from Sigma-Aldrich Inc., St. Louis, MO, USA; 5-fluorouracil (5-FU) from Kyowa, Tokyo, Japan; cisplatin (CDDP) from Nichi-Iko Pharmaceutical Co. Ltd., Toyama, Japan; carboplatin (CBDCA) from Sawai Pharmaceutical Co. Ltd., Osaka, Japan; Paclitaxel (PTX) from Nipro Corporation, Osaka, Japan; dimethyl sulfoxide (DMSO) and actinomycin D (Act. D) from Wako Pure Chem. Ind., Osaka, Japan. Regarding consumables, 100-mm treated culture dishes were purchased from TrueLine, Nippon Genetics Co., Ltd, Tokyo, Japan and 96-well plates from Techno Plastic Products AG, Trasadingen, Switzerland.

Synthesis of guaiazulene-3-carboxylate derivatives. Methyl guaiazulene-3-carboxylate [**1**], ethyl guaiazulene-3-carboxylate [**2**], *n*-propyl guaiazulene-3-carboxylate [**3**], isopropyl guaiazulene-3-carboxylate [**4**], *n*-butyl guaiazulene-3-carboxylate [**5**], 2-methoxyethyl guaiazulene-3-carboxylate [**6**], 2-ethoxyethyl guaiazulene-3-carboxylate [**7**], 2-hydroxyethyl guaiazulene-3-carboxylate [**8**], 2-(2-hydroxyethoxy)ethyl guaiazulene-3-carboxylate

Table I. *Cytotoxicity and tumor-specificity (evaluated by TS and PSE values) of 12 guaiazulene-3-carboxylate derivatives against human oral squamous cell carcinoma (OSCC) cell lines and human normal oral cells (normal).*

Compound	CC_{50}**		TS		PSE		T***	N***	T-N***
	OSCC	Normal	TS_{mean}	$TS_{(HGF/Ca9-22)}$	PSE_{mean}	$PSE_{(HGF/Ca9-22)}$			
1*	154.5±29.8	192.9±33.9	1.3±0.1	1.2±0.4	0.8±0.2	0.9±0.3	0.81093	0.71479	0.09613
2	137.7±8.6	217.6±41.3	1.6±0.3	1.5±0.6	1.1±0.2	1.2±0.5	0.86125	0.66258	0.19867
3*	54.2±26.0	102.4±35.2	2.0±0.4	2.0±1.0	4.9±3.9	6.1±6.5	1.26527	0.98981	0.27546
4*	45.0±7.1	82.0±14.4	1.8±0.1	1.7±0.8	4.1±0.6	3.9±1.9	1.34630	1.08584	0.26046
5*	78.7±5.2	225.9±12.3	2.9±0.3	2.2±1.3	3.7±0.6	2.9±1.9	1.10286	0.64636	0.45650
6*	34.8±5.6	155.6±29.3	**4.5±0.2**	**4.4±3.3**	**13.0±1.9**	**13.8±10.1**	1.45959	0.80807	**0.65151**
7	28.0±2.1	125.2±55.3	**4.4±1.7**	**3.7±3.5**	**15.5±5.2**	**16.1±15.5**	1.55350	0.90238	**0.65112**
8*	50.5±3.9	97.9±16.8	2.0±0.4	2.1±1.4	3.9±1.0	4.7±3.4	1.29614	1.00898	0.28716
9*	43.3±16.0	92.9±34.3	2.1±0.0	2.8±1.5	5.6±2.6	10.3±4.7	1.36349	1.03337	0.33013
10*	26.9±1.4	65.0±11.4	2.4±0.4	3.6±2.5	9.0±1.5	18.1±13.5	1.57208	1.18668	0.38540
11*	17.7±5.2	31.8±4.9	1.9±0.4	1.7±0.4	11.6±6.0	9.3±4.7	1.75417	1.49840	0.25576
12*	19.7±1.4	34.1±1.3	1.7±0.1	1.8±0.3	8.8±0.9	9.7±3.0	1.70885	1.46693	0.24192
5-FU	63.8±3.8	578.7±328.7	8.8±4.6	51.6±13.0	13.4±6.5	895.6±776.5	1.19510	0.23770	0.95741
CDDP	2.6±1.2	4.0±1.2	2.2±1.5	1.4±0.6	136.3±117.3	56.5±28.7	2.56540	2.39794	0.16746
CBDCA	3.6±0.8	8.1±3.1	2.4± 1.1	1.6±0.6	69.3±38.1	34.5±14.5	2.44186	2.09691	0.34495

5-FU: Fluorouracil; CDDP: cisplatin; CBDCA, carboplatin; TS: tumor-selectivity index; PSE: potency-selectivity expression; TSmean: CC_{50} (normal)/CC_{50} (OSCC); TS(HGF/ Ca9-22): CC_{50} (HGF)/CC_{50} (Ca9-22); PSE_{mean}: [$TS_{(mean)}$/CC_{50} (OSCC)]×100; $PSE_{(HGF/Ca9-22)}$: [$TS_{(HGF/Ca9-22)}$/CC_{50} (Ca9-22)]×100. Bold values represent the highest values of TS, PSE and T-N among 12 compounds. *Significant difference ($p<0.05$) between the mean of CC_{50} of OSCC cells and that of normal cells. **Presented as mean±SD. ***The negative log CC_{50} (pCC_{50}) values for tumor and normal cells, respectively. The difference (T–N) was used as a tumor-selectivity index. Each value represents the mean±SD from three independent experiments that were done in triplicate.

[**9**], 2-aminoethyl guaiazulene-3-carboxylate [**10**], 3-aminoprpyl guaiazulene-3-carboxylate [**11**], 4-aminobutyl guaiazulene-3-carboxylate [**12**] (Figure 1G) were synthesized, according to previous reports (6, 17, 18). *N*-(2-methoxyethyl)guaiazulenecarboxamide [**X**] was synthesized as previously described (15). All compounds were dissolved in DMSO at 40 mM and stored at –20˚C before use.

Cell culture. Human normal oral cells [gingival fibroblast (HGF), periodontal ligament fibroblast (HPLF), pulp cell (HPC)] (19) at 12~20 population doubling level (PDL) and OSCC cell lines (Ca9-22, HSC-2, HSC-3, HSC-4) (Riken Cell Bank, Tsukuba, Japan) were cultured at 37˚C in DMEM supplemented with 10% heat-inactivated FBS and antibiotics under humidified 5% CO_2 atmosphere, as described previously (14-16).

Assay for cytotoxic activity. Cells were inoculated at 2×10^3 cells/0.1 ml in a 96-microwell plate. After 48 h, the medium was replaced with 0.1 ml of fresh medium containing various concentrations of test compounds. Control cells were treated with the same amounts of DMSO present in each diluent solution. Cells were incubated for 48 h and the relative viable cell number was then determined by the MTT method, as described previously (14-16). The CC_{50} was determined from the dose–response curve of triplicate samples.

Calculation of tumor-selectivity index (TS). $TS_{(mean)}$ was calculated as the ratio of the mean CC_{50} value for the human normal oral cells (HGF+HPLF+HPC) to that for the OSCC cell lines (Ca9-22+HSC-2+HSC-3+HSC-4). Moreover, TS was calculated for cells derived from gingival tissue (20), and as the ratio of CC_{50} (HGF) to CC_{50} (Ca9-22) ($TS_{(HGF/Ca9-22)}$).

Calculation of potency-selectivity expression (PSE). PSE was calculated by the formula: (TS/CC_{50}) ×100 (11, 12).

Cell cycle analysis. Cells (approximately 10^6 cells) were harvested, fixed, treated with ribonuclease A, stained propidium iodide, filtered through cell strainers and then were subjected to cell sorting (SH800 Series, SONY Imaging Products and Solutions Inc., Atsugi, Kanagawa, Japan) and cell cycle analysis (Cell Sorter Software version 2.1.2., SONY Imaging Products and Solutions Inc), as described previously (16).

Calculation of chemical descriptors. pCC_{50} (*i.e.*, the –log CC_{50}) was used for the comparison of the cytotoxicity between the compounds, since the CC_{50} values had a distribution pattern close to a logarithmic normal distribution. The mean pCC_{50} values for normal cells and tumor cell lines were defined as N and T, respectively (15, 16) (Table II). The 3D-structure of each chemical structure was drawn by Marvin Sketch (MarvinSketch 18.10.0, ChemAxon, Budapest, Hungary, http://www.chemaxon.com), and optimized by CORINA Classic (Molecular Networks GmbH, Nürnberg, Germany) with forcefield calculations (amber-10: EHT) in Molecular Operating Environment (MOE) version 2019.0101 (Chemical Computing Group Inc., Quebec, Canada) and Dragon (Dragon 7 version 7.0.2, Kode srl., Pisa, Italy).

Statistical analysis. Each experimental value was expressed as the mean±standard deviation (SD) of triplicate or quadruplicate measurements. The statistical analysis was performed using one-way analysis of variance (ANOVA) followed by Bonferroni's post-hoc test for multiple comparisons. The correlation between chemical

Table II. *Top six chemical descriptors that correlate with cytotoxicity to tumor cells, normal cells and tumor-specificity (having the highest r^2 values).*

	Descriptor	Source	Meaning	Category	Explanation
T	BCUT_ SLOGP_0	MOE	Topological shape	Adjacency and distance matrix descriptors	The BCUT descriptors using atomic contribution to logP (using the Wildman and Crippen SlogP method) instead of partial charge.
	Mi	Dragon	Ionization potential	Constitutional indices	Mean first ionization potential (scaled on Carbon atom)
	Mor24e	Dragon	3D shape and electric state	3D-MoRSE descriptors	Signal 11/weighted by Sanderson electronegativity
	C%	Dragon	Percentage of C atoms	Constitutional indices	Percentage of C atoms
	Mor24i	Dragon	3D shape and ionization potential	3D-MoRSE descriptors	Signal 10/weighted by ionization potential
	DISPi	Dragon	3D shape, size and ionization potential	Geometrical descriptors	Displacement value/weighted by ionization potential
N	vsurf_Wp2	MOE	3D shape and polarizability	Surface area, Volume and Shape descriptors	Polar volume
	vsurf_IW1	MOE	3D shape and hydrophilicity	Surface area, Volume and Shape descriptors	Hydrophilic integy moment
	h_logD	MOE	Lipophilicity	Physical properties	The octanol/water distribution coefficient at pH 7.
	vsurf_Wp3	MOE	3D shape and polarizability	Surface area, Volume and Shape descriptors	Polar volume
	RDF010s	Dragon	3D shape, size and electric state	RDF descriptors	Radial Distribution Function - 010/weighted by I-state
	BCUT_ SLOGP_0	MOE	Topological shape	Adjacency and distance matrix descriptors	The BCUT descriptors using atomic contribution to logP (using the Wildman and Crippen SlogP method) instead of partial charge.
T-N	MEcc	Dragon	3D shape	Geometrical descriptors	Molecular eccentricity
	L3s	Dragon	3D shape, size and electric state	WHIM descriptors	2nd component size directional WHIM index/weighted by I-state
	SpMAD_G/D	Dragon	3D shape and size	3D matrix-based descriptors	Spectral mean absolute deviation from distance/distance matrix
	L3m	Dragon	3D shape, size and electric state	WHIM descriptors	3rd component size directional WHIM index/weighted by mass
	H2i	Dragon	3D shape and ionization potential	GETAWAY descriptors	H autocorrelation of lag 8/weighted by ionization potential
	TDB10i	Dragon	3D shape and ionization potential	3D autocorrelations	3D topological distance-based descriptors - lag 10 weighted by ionization potential

descriptors and cytotoxicity or tumor specificity index was investigated using linear regression analyses. The significance level was set at $p<0.05$. Statistical analysis was performed using the JMP Pro version 14.3.0 software (SAS Institute Inc., Cary, NC, USA).

Results

Cytotoxicity and tumor-specificity. Twelve guaiazulene-3-carboxylate derivatives used in this study were classified into four groups: alkyl guaiazulene-3-carboxylates **[1-5]**, alkoxyl guaiazulene-3-carboxylates **[6, 7]**, hydroxyalkyl guaiazulene-3-carboxylates **[8, 9]** and aminoalkyl guaiazulene-3-carboxylates **[10-12]** (Figure 1G). We compared their cytotoxic activity against four human oral squamous cell carcinoma (OSCC) cell lines (Ca9-22, HSC-2, HSC-3, HSC-4) and three normal oral cells (HGF, HPLF, HPC), by comparing the 50% cytotoxic concentration (CC_{50}) determined from the dose-response curve (Table I). We have adopted 48 h treatment time, based on our observation that significant ($p<0.05$) cytotoxicity of compounds [**6, 7**] appeared 3 h after treatment, reaching the plateau level after 24~48 h (Figure 2). We have repeated the same experiments 3 times. The mean values of CC_{50}, tumor-selectivity index (TS), and potency-selectivity expression (PSE) of these twelve compounds, as well as of positive controls (5-FU, CDDP, and CBDCA) obtained from these 3 independent experiments are listed in Table I. Most of the compounds [**1, 3, 4-6, 8-12**] showed significantly higher cytotoxicity against OSCC cell lines, compared to normal cells ($p<0.05$). Among the 12 studied guaiazulene-3-carboxylates, two alkoxyl guaiazulene-3-carboxylates [**6, 7**] ($TS_{mean}=4.4\pm0.2$; PSE=13.0±1.9) showed the highest TS values than five alkyl guaiazulene-3-carboxylates [**1-5**], two hydroxyalkyl guaiazulene-3-carboxylates [**8, 9**], and three aminoalkyl guaiazulene-3-carboxylates [**10-12**] (Table I). Moreover, both

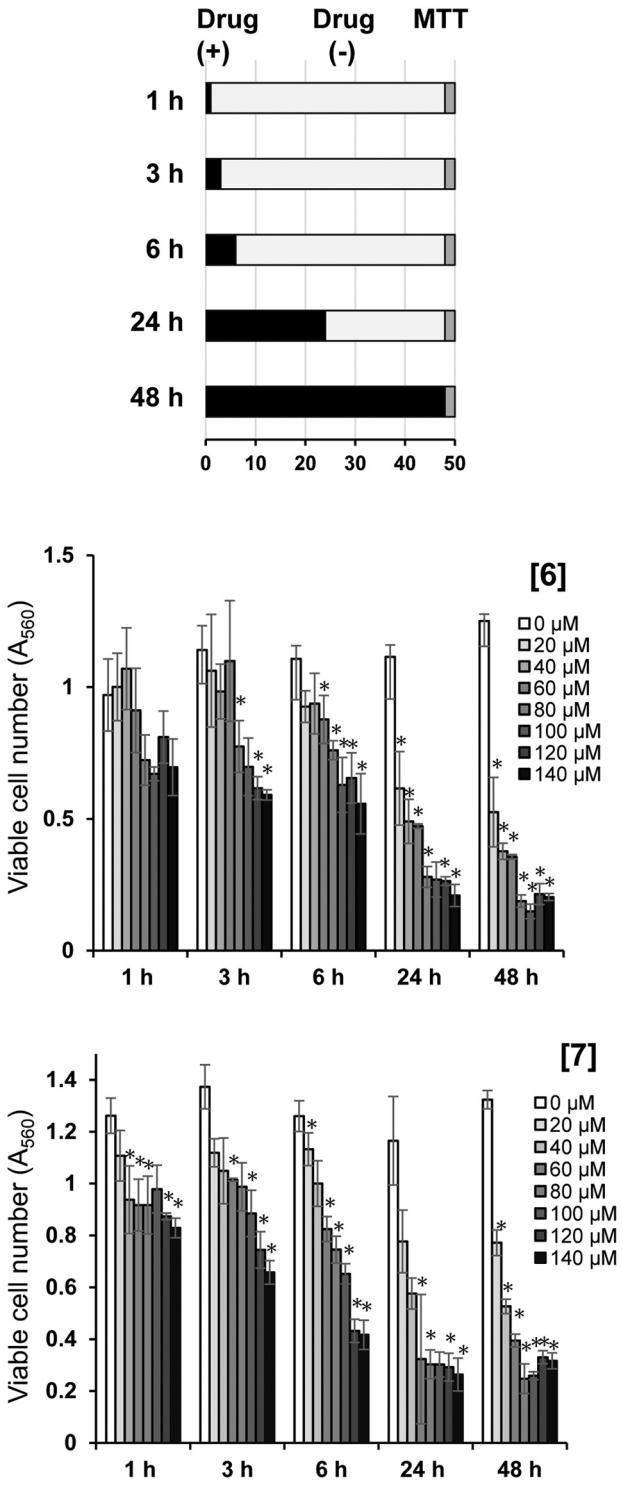

Figure 2. *Time- and dose-response of cytotoxicity induction by [**6**] and [**7**]. HSC-2 cells were incubated for 1, 3, 6, 24 or 48 h with the indicated concentrations of [**6**] or [**7**], and then the viable cell number was determined by MTT method. Each value represents mean±SD of triplicate assays. The differences between control and treated groups were evaluated by one-way analysis of variance (ANOVA) followed by Bonferroni's post-hoc test for multiple comparisons. *p<0.05 compared with control.*

[**6, 7**] showed higher TS value than CDDP and CBDCA (TS_{mean}=2.2±1.5 and 2.4±1.1, respectively), and had $PSE_{(mean)}$ values comparable to that of 5-FU (13.4±6.5). Regarding $TS_{(HGF/Ca9-22)}$ and $PSE_{(HGF/Ca9-22)}$, high SD values were observed, possibly due to a cytostatic, rather than cytotoxic inhibition of cell proliferation, causing variations of CC_{50} values in each experiment (Table I).

Induction of apoptosis and G_2/M arrest. Light microscopical observation (Figure 3A) revealed that HSC-2 cells treated for 48 h with 20 μM of either [**6**] or [**7**] (slightly lower concentration of their CC_{50}: 34.8 and 28.0 μM, Table I) were a mixture of shrunken and spread cells. Cell cycle analysis demonstrated that when compared to the control, [**6, 7**] significantly (p<0.05) reduced the G_1 cell population, while increased the $subG_1$ and G_2/M phase cells, regardless of treatment time (24 h and 48 h) (Figure 3B, 3C). Actinomycin D (Act. D) increased more the percentage of $subG_1$ cell population (p<0.05), but slightly reduced (p<0.05) the G_2/M phase cells at 24 h (Figure 3B, 3C).

Computational analysis. The number of descriptors calculated from MOE and dragon were 344 and 5,255, respectively. As a result of excluding duplicates or descriptors with standard deviation of 0, the number of descriptors reduced to 264, 2,808, respectively. Among a total of 3,072 descriptors, the top six descriptors that showed the highest correlation coefficient (r^2) to T, N and T-N are listed in Table II.

Cytotoxicity against human OSCC cell lines was correlated with descriptors BCUT_SLOGP_0 (r^2=0.841, p<0.0001) (topological shape), Mi (r^2=0.785, p=0.0001) (ionization potential), Mor24e (r^2=0.757, p=0.0002) (3D shape and electric state), C% (r^2=0.751, p=0.0003) (percentage of C atoms), Mor24i (r^2=0.737, p=0.0003) (3D shape and ionization potential) and DISPi (r^2=0.734, p=0.0004) (3D shape, size and ionization potential) (Figure 4).

Cytotoxicity against human normal oral mesenchymal cells was correlated with descriptors vsurf_Wp2 (r^2=0.783, p=0.0001) (3D shape and polarizability), vsurf_IW1 (r^2=0.753, p=0.0003) (3D shape and hydrophilicity), h_logD (r^2=0.751, p=0.0003) (lipophilicity), vsurf_Wp3 (r^2=0.740, p=0.0003) (3D shape and polarizability), RDF010s (r^2=0.730, p=0.0004) (3D shape, size and electric state), and BCUT_SLOGP_0 (r^2=0.678, p=0.0010) (topological shape) (Figure 5).

Tumor-specificity was correlated with descriptors MEcc (r^2=0.696, p=0.0007) (3D shape), L3s (r^2=0.692, p=0.0008) (3D shape, size and electric state), SpMAD_G/D (r^2=0.678, p=0.0010) (3D shape and size), L3m (r^2=0.649, p=0.0016) (3D shape, size and electric state), H2i (r^2=0.648, p=0.0016) (3D shape and ionization potential) and TDB10i (r^2=0.646, p=0.0016) (3D shape and ionization potential) (Figure 6).

These data suggest that both tumor-specificity and cytotoxicity of guaiazulene-3-carboxylate against OSCC

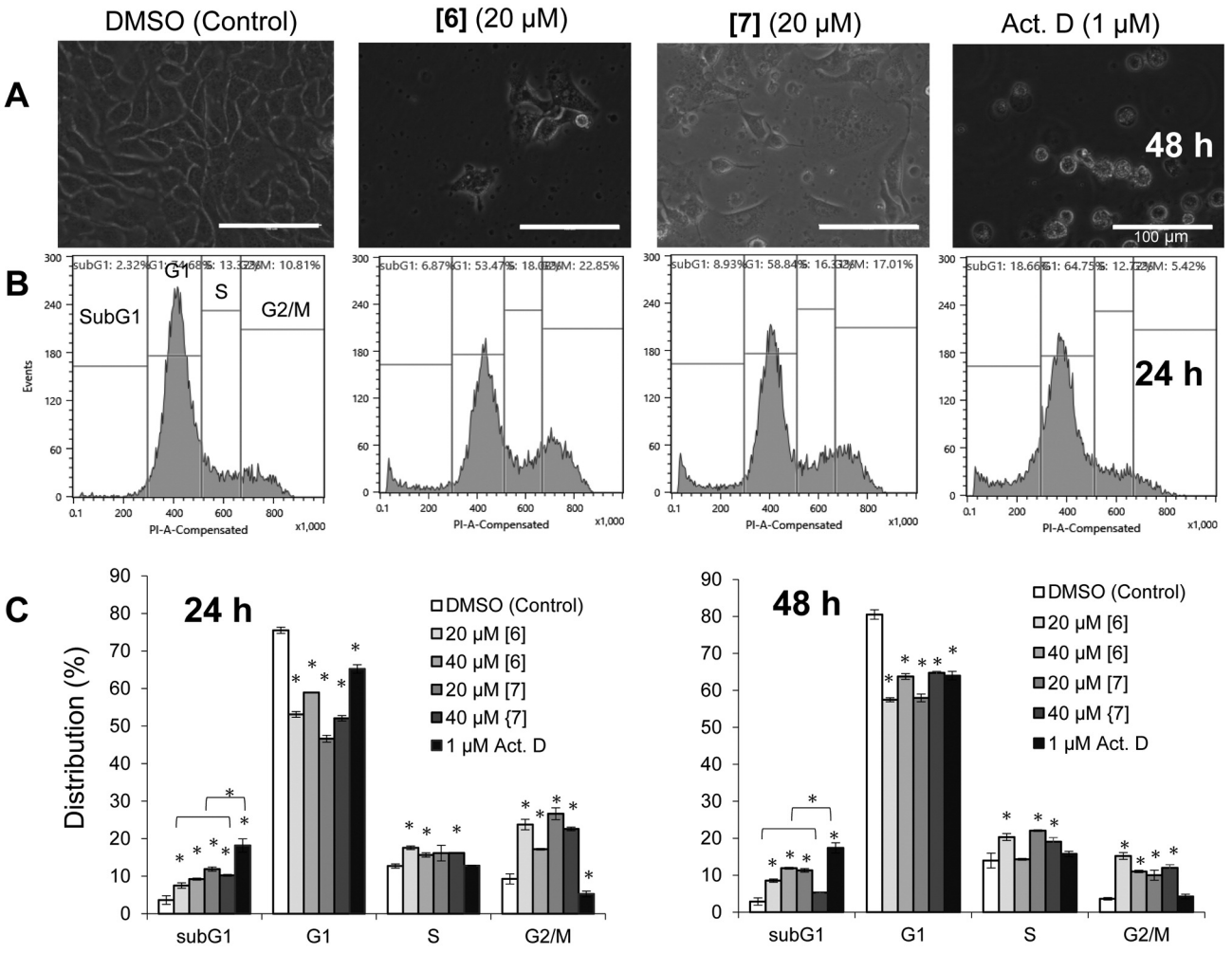

Figure 3. *Production of subG$_1$ and G$_2$/M cell populations by [**6, 7**]. HSC-2 cells were treated for 48 h or 24 h without (control) or with 20 μM [**6**], 20 μM [7] or 1 μM actinomycin D (Act. D) and then cell morphology (A) and cell cycle distribution (assessed by cell sorter) (B) were investigated. (C) Summary of the data of cell cycle distribution after 24 and 48 h. Each value represents mean±SD of triplicate assays. *p<0.05: Statistical significance from control. Scale of bar in (A): 100 μm.*

correlate with 3D shape, electric state, and especially ionization potential.

Discussion

The present study demonstrated that among twelve guaiazulene-3-carboxylates, two alkoxyl guaiazulene-3-carboxylates [**6, 7**] showed higher tumor-specificity than five alkyl [**1-5**] and two hydroxyalkyl [**8, 9**] guaiazulene-3-carboxylates and three aminoalkyl guaiazulene-3-carboxylate carboxamides [**10-12**] (Table I). Both [**6, 7**] showed higher TS value than CDDP and CBDCA, and having comparable PSE value with 5-FU (Table I). Higher TS of [**6, 7**] might be explained by their 3D shape, electric state and especially ionization potential (Figure 6). This point was confirmed by the fact that when carboxylate portion in [**6**] was replaced with amide (*N*-(2-methoxyethyl)guaiazulenecarboxamide [**X**]), both TS and PSE were reduced (Figure 7). Guaiazulene has been reported to induce apoptosis in normal HGF (21). Therefore, compounds with much higher tumor-specificity should be synthesized.

PubMed search demonstrated that no paper published on the G$_2$/M arrest by guaiazulene. Therefore, the present study demonstrated for the first time that [**6, 7**] induced cell shrinkage and subG$_1$ cell accumulation (one of the markers of apoptosis) (22, 23), as well as G$_2$/M cell accumulation (indication of mitotic arrest). We have recently reported that 7-isopropyl-3-methyl-*N*-propylazulene-1-carboxamide and 2-methoxy-*N*-pentylazulene-1-carboxamide, both of which do not have

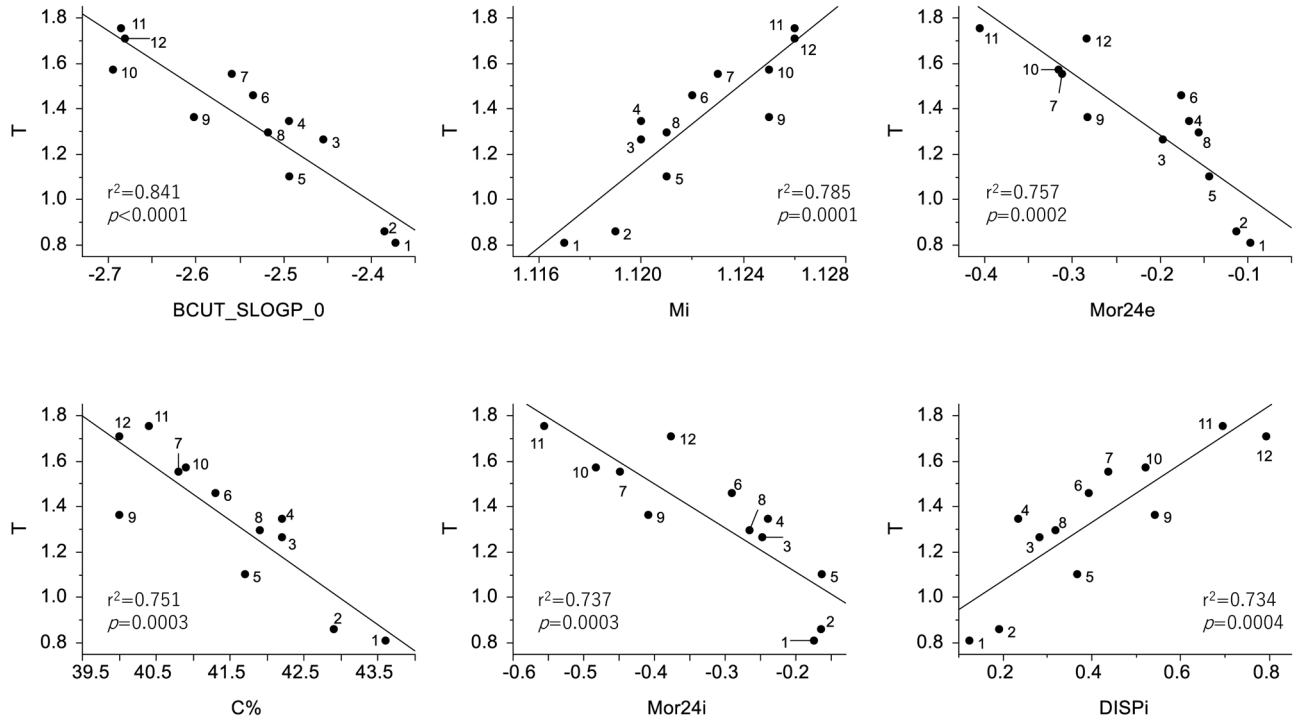

Figure 4. *Determination of coefficient between chemical descriptors and cytotoxicity of 12 guaiazulene-3-carboxylate derivatives against tumor cells (defined as T). The mean (pCC_{50} i.e., the $-\log CC_{50}$) values for tumor cell lines were defined as T.*

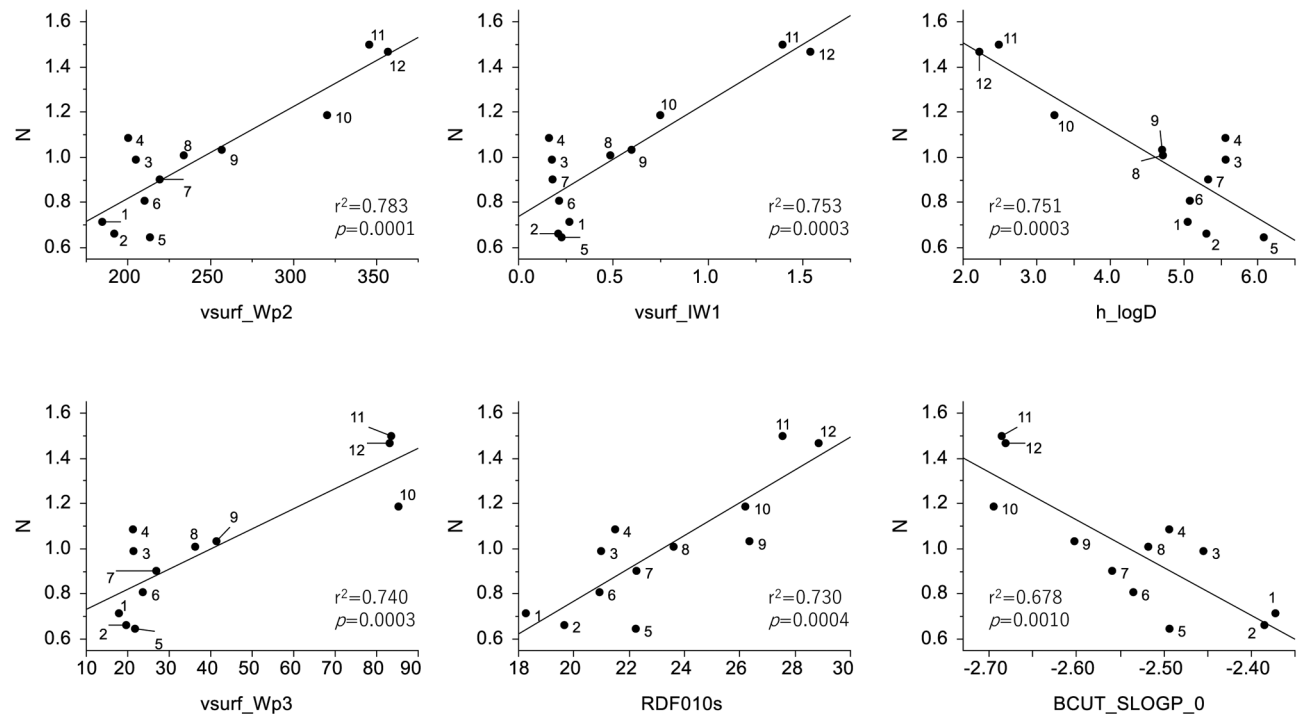

Figure 5. *Determination of coefficient between chemical descriptors and cytotoxicity of 12 guaiazulene-3-carboxylate derivatives against normal cells (defined as N). The mean (pCC_{50} i.e., the $-\log CC_{50}$) values for normal cells were defined as N.*

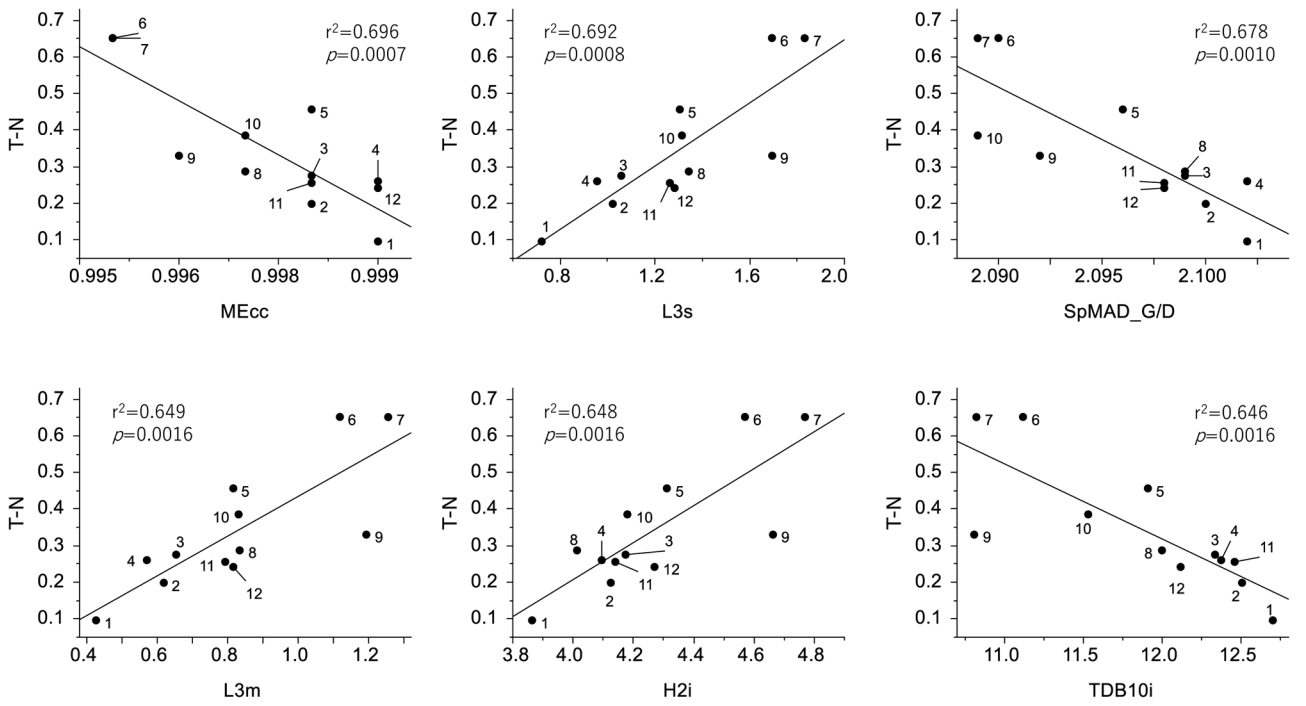

Figure 6. *Determination of coefficient between chemical descriptors and tumor specificity of 12 guaiazulene-3-carboxylate derivatives (defined as T–N).*

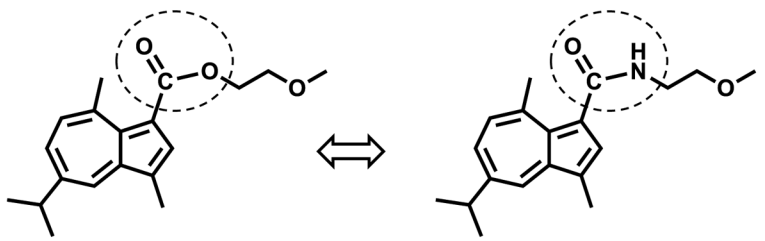

6: TS=8.5 (D/B) **; 9.0** (C/A)
PSE=23.3 [100(D/B²)]; **27.6** [100(C/A²)]

X: TS=4.1(D/B**); 4.2 (**C/A**)**
PSE=7.1 [100(D/B²)];**7.8** [100(C/A²)]

	CC_{50} (μM)												
	Human OSCC cell lines					Human normal oral cells				TS		PSE	
	Ca9-22	HSC-2	HSC-3	HSC-4	mean	HGF	HPLF	HPC	mean				
	(A)				(B)	(C)			(D)	D/B	C/A	100(D/B²)	100(C/A²)
6	32.7	16.7	49.7	43.0	36.4	294.3	328.2	304.8	309.1	8.5	9.0	23.3	27.6
X	54.3	54.1	69.0	52.0	58.4	230.6	261.1	232.7	241.5	4.1	4.2	7.1	7.8

Figure 7. *Comparison of tumor-specificity (TS) values between [**6**] and N-(2-methoxyethyl)guaiazulenecarboxamide [**X**]. Four OSCC cell lines and three normal cells were incubated for 48 h with the indicated concentrations of [**6**] or [**X**] that was synthesized as previously described (15), and then TS and potency-selectivity expression (PSE) values were determined. Each value represents mean of triplicate assays.*

guaiazulene structure, did not induce the accumulation at G_2/M, although they induced apoptosis in HSC-2 cells (16). Taken together, the presence of guaiazulene structure may be involved in G_2/M arrest induction; however, further study is required to confirm the induction of apoptosis markers by [**6, 7**] and investigate the possible link of G_2/M arrest and apoptosis induction.

We have recently reported that several G_2/M blockers such as taxanes paclitaxel [Taxol®, the first microtubule stabilizing agent (24)] and docetaxel (25), and 3-styrylchromone derivatives [7-methoxy-3-[(1*E*)-2-phenylethenyl]-4*H*-1-benzopyran-4-one, 3-[(1*E*)-2-(4-hydroxyphenyl)ethenyl]-7-methoxy-4*H*-1-benzopyran-4-one] show very high TS values (>7267, >86122, 301 and 182, respectively) (26). However, many reports, including ours, demonstrated that microtubule-targeted agents have potent neurotoxicity, adversely affecting the quality of life of patients on a long-term basis (27-30). We have also reported that doxorubicin induced very potent keratinocyte toxicity by inducing apoptosis, characterized by the loss of cell surface microvilli, chromatin condensation, nuclear fragmentation and caspase-3 activation (31). Therefore, the possible side effects of guaiazulene-3-carboxylate derivatives such as neurotoxicity and keratinocyte toxicity should be evaluated.

In conclusion, the present study demonstrated for the first time that two guaiazulene-3-carboxylate derivatives with alkoxy group at the end of sidechain [**6, 7**] showed highest TS against OSCC cell lines, among 12 related compounds, and induced subG_1 and G_2/M arrest. TS was correlated with chemical descriptors that explain the 3D shape, electric state, and ionization potential. These two compounds can be potential candidates of lead compound for manufacturing new type of anticancer drugs. Further study is ongoing by our team, regarding combination of [**6**] or [**7**] and anticancer drugs against the human OSCC HSC-2 cell line.

Conflicts of Interest

The Authors confirm that there are no known conflicts of interest associated with this publication and there was no significant financial support for this work that could have influenced its outcome.

Author's Contributions

M.T., S.N. performed all experiments. M.F. synthesized samples. N.O., K.B., Y.I. and H.S. performed the cell culture and apoptosis assays. J.N. and Y.U. performed the QSAR analysis. H.S., M.H. and H.W. wrote and reviewed the manuscript.

Acknowledgements

This work was partially supported by KAKENHI from the Japan Society for the Promotion of Science (JSPS) (16K11519).

References

1 Nozoe T and Asao T: Azulenes and heptafulvenes. *In*: Dai-Yuki Kagaku. Kotake M (ed.), Tokyo, Asakura-Shoten, Vol.13, pp. 439-534, 1960 (in Japanese).

2 Nozoe T, Breslow R, Hafner K, Ito S and Murata I: Topics in Nonbenzenoid Aromatic Chemistry. Tokyo, Hirokawa Publ. Co., Vol I: pp. 1-295, 1973.

3 Nozoe T, Breslow R, Hafner K, Ito S and Murata I: Topics in Nonbenzenoid Aromatic Chemistry. Tokyo, Hirokawa Publ. Co., Vol II: *pp*. 1-379, 1977.

4 Zeller KP: Methoden der organischen chemie. New York, Houben-Weyl, Band V/2c, pp. 127-418, 1985.

5 Nihei S, Sato J, Komatsu H, Ishida K, Kimura T, Tomita T and Kudo K: The efficacy of sodium azulene sulfonate L-glutamine for managing chemotherapy-induced oral mucositis in cancer patients: a prospective comparative study. J Pharm Health Care Sci *4*: 20, 2018. PMID: 30123519. DOI: 10.1186/s40780-018-0114-2

6 Matsumoto K, Matsuo K, Yatagai N, Enomoto Y, Shigeoka M, Hasegawa T, Suzuki H and Komori T: Clinical evaluation of CO_2 laser vaporization therapy for oral lichen planus: A single-arm intervention study. Photobiomodul Photomed Laser Surg *37(3):* 175-181, 2019. PMID: 31050948. DOI: 10.1089/photob.2018.4559

7 Ayaz F, Yuzer A, Ince T and Ince M: Anti-cancer and anti-Inflammatory activities of bromo- and cyano-substituted azulene derivatives. Inflammation, 2020. DOI: 10.1007/s10753-020-01186-0

8 Sakai H and Misawa M: Effect of sodium azulene sulfonate on capsaicin-induced pharyngitis in rats. Basic Clin Pharmacol Toxicol *96(1)*: 54-59, 2005. PMID: 15667596. DOI: 10.1111/j.1742-7843.2005.pto960108.x

9 Kourounakis AP, Rekka EA and Kourounakis PN: Antioxidant activity of guaiazulene and protection against paracetamol hepatotoxicity in rats. J Pharm Pharmacol *49(9):* 938-942, 1997. PMID: 9306266. DOI: 10.1111/j.2042-7158.1997.tb06140.x

10 Pratsinis H and Haroutounian SA: Synthesis and antioxidant activity of 3-substituted guaiazulene derivatives. Nat Prod Lett *16(3):* 201-205, 2002. PMID: 12049221. DOI: 10.1080/1057563 0290013585

11 Mangkhalthon AP, Teerakapong A, Tippayawat P, Morales NP, Morkmued S, Puasiri S, Priprem A and Damrongrungruang T: Anti-inflammatory effect of photodynamic therapy using guaiazulene and red lasers on peripheral blood mononuclear cells. Photodiagnosis Photodyn Ther 101747, 2020. PMID: 32200021. DOI: 10.1016/j.pdpdt.2020.101747

12 Kakei T, Matsumoto M, Kojima K, Suzuki R and Narita R: Guaiazulene mouthwash for diseases of the oral mucosa. Shikai Tenbo *63(4)*: 843-849, 1984. PMID: 6591496.

13 Zhai W, Liu J, Liu Q, Wang Y and Yang D: Rapid identification and global characterization of multiple constituents from the essential oil of Cortex Dictamni based on GC-MS. J Sep Sci *40(12):* 2671-2681, 2017. PMID: 28493524. DOI: 10.1002/jssc.201700072

14 Uehara M, Minemura H, Ohno T, Hashimoto M, Wakabayashi H, Okudaira N and Sakagami H: *In vitro* antitumor activity of alkylaminoguaiazulenes. In Vivo *32(3):* 541-547, 2018. PMID: 29695558. DOI: 10.21873/invivo.11273

15 Wada T, Maruyama R, Irie Y, Hashimoto M, Wakabayashi H, Okudaira N, Uesawa Y, Kagaya H and Sakagami H: *In vitro*

anti-tumor activity of azulene amide derivatives. In Vivo *32(3):* 479-486, 2018. PMID: 29695549. DOI: 10.21873/invivo.11264

16 Imanari K, Hashimoto M, Wakabayashi H, Okudaira N, Bandow K, Nagai J, Tomomura M, Tomomura A, Uesawa Y and Sakagami H: Quantitative structure-cytotoxicity relationship of azulene amide derivatives. Anticancer Res *39(7):* 3507-3518, 2019. PMID: 31262875. DOI: 10.21873/anticanres.13497

17 Anderson AG and Anderson RG: The reaction of azulenes with trifluoro- and trichloroacetic anhydride. J Org Chem *27(10):* 3578-3581, 1962. DOI: 10.1021/jo01057a044

18 Okajima T and Kurokawa S: Facile conversion of 1-methyl group of guaiazuleue into 1-formyl group. Chem Lett *26(1):* 69-70, 1997. DOI: 10.1246/cl.1997.69

19 Kantoh K, Ono M, Nakamura Y, Nakamura Y, Hashimoto K, Sakagami H and Wakabayashi H: Hormetic and anti-radiation effects of tropolone-related compounds. In Vivo *24(6):* 843-851, 2010. PMID: 21164042.

20 Horikoshi M, Kimura Y, Nagura H, Ono T and Ito H: A new human cell line derived from human carcinoma of the gingiva. I. Its establishment and morphological studies. Nihon Koku Geka Gakkai Zasshi *20(2):* 100-106, 1974. PMID: 4549822. DOI: 10.5794/jjoms.20.100

21 Fiori J, Teti G, Gotti R, Mazzotti G and Falconi M: Cytotoxic activity of guaiazulene on gingival fibroblasts and the influence of light exposure on guaiazulene-induced cell death. Toxicol In Vitro *25(1):* 64-72, 2011. PMID: 20854889. DOI: 10.1016/j.tiv.2010.09.008

22 Majno G and Joris I: Apoptosis, oncosis, and necrosis. An overview of cell death. Am J Pathol *146(1):* 3-15, 1995. PMID: 7856735.

23 Wlodkowic D, Telford W, Skommer J and Darzynkiewicz Z: Apoptosis and beyond: cytometry in studies of programmed cell death. Methods Cell Biol *103:* 55-98, 2011. PMID: 21722800. DOI: 10.1016/B978-0-12-385493-3.00004-8

24 Yang CH and Horwitz SB: Taxol®: The first microtubule stabilizing agent. Int J Mol Sci *18(8)*: 1733, 2017. PMID: 28792473. DOI: 10.3390/ijms18081733

25 Iijima Y, Bandow K, Sano M, Hino S, Kaneko T, Horie N and Sakagami H: *In vitro* assessment of antitumor potential and combination Effect of classical and molecular-targeted anticancer drugs. Anticancer Res *39(12):* 6673-6684, 2019. PMID: 31810932. DOI: 10.21873/anticanres.13882

26 Takao K, Hoshi K, Sakagami H, Shi H, Bandow K, Nagai J, Uesawa Y, Tomomura A, Tomomura M and Sugita Y: Further quantitative structure-cytotoxicity relationship analysis of 3-styrylchromones. Anticancer Res *40(1):* 87-95, 2020. PMID: 31892556. DOI: 10.21873/anticanres.13929

27 da Costa R, Passos GF, Quintão NLM, Fernandes ES, Maia JRLCB, Campos MM and Calixto JB: Taxane-induced neurotoxicity: pathophysiology and therapeutic perspectives. Br J Pharmacol, 2020. PMID: 32352155. DOI: 10.1111/bph.15086

28 Pittman SK, Gracias NG and Fehrenbacher JC: Nerve growth factor alters microtubule targeting agent-induced neurotransmitter release but not MTA-induced neurite retraction in sensory neurons. Exp Neurol *279:* 104-115, 2016. PMID: 26883566. DOI: 10.1016/j.expneurol.2016.02.010

29 Rovini A, Savry A, Braguer D and Carré M: Microtubule-targeted agents: when mitochondria become essential to chemotherapy. Biochim Biophys Acta *1807(6):* 679-688, 2011. PMID: 21216222. DOI: 10.1016/j.bbabio.2011.01.001

30 Iijima Y, Bandow K, Amano S, Sano M, Hino S, Kaneko T, Horie N and Sakagami H: Protection of bortezomib-induced neurotoxicity by antioxidants. Anticancer Res *40(7)*, 2020.

31 Sakagami H, Okudaira N, Masuda Y, Amano O, Yokose S, Kanda Y, Suguro M, Natori T, Oizumi H and Oizumi T: Induction of apoptosis in human oral keratinocyte by doxorubicin. Anticancer Res *37(3)*: 1023-1029, 2017. PMID: 28314260. DOI: 10.21873/anticanres.11412

Received May 9, 2020
Revised June 7, 2020
Accepted June 24, 2020